

bradscholars

Size effect on shear strength of FRP reinforced concrete beams

Item Type	Article
Authors	Ashour, Ashraf;Kara, Ilker F.
Citation	Ashour AF and Kara IF (2014) Size Effect on Shear Strength of FRP Reinforced Concrete Beams. Composites: Part B, 60: 612-620.
DOI	https://doi.org/10.1016/j.compositesb.2013.12.002
Rights	© 2014 Elsevier. Reproduced in accordance with the publisher's self-archiving policy.
Download date	2026-04-12 08:37:39
Link to Item	http://hdl.handle.net/10454/7606

The University of Bradford Institutional Repository

<http://bradscholars.brad.ac.uk>

This work is made available online in accordance with publisher policies. Please refer to the repository record for this item and our Policy Document available from the repository home page for further information.

To see the final version of this work please visit the publisher's website. Available access to the published online version may require a subscription.

Link to original published version: <http://dx.doi.org/10.1016/j.compositesb.2013.12.002>

Citation: Ashour AF and Kara IF (2014) Size Effect on Shear Strength of FRP Reinforced Concrete Beams. Composites: Part B, 60: 612-620.

Copyright statement: © 2014 Elsevier. Reproduced in accordance with the publisher's self-archiving policy.



SIZE EFFECT ON SHEAR STRENGTH OF FRP REINFORCED CONCRETE BEAMS

Ashraf F. Ashour^a, Ilker Fatih Kara^{b,*}

^a School of Engineering, Design and Technology, University of Bradford, BD7 1DP, UK

^b Civil Engineering Department, Nigde University, 51245, Nigde, Turkey

* Corresponding author, Email: ifkara@nigde.edu.tr, Tel: +90 388 2252293, Fax: +90 388 225 0112

ABSTRACT

This paper presents test results of six concrete beams reinforced with longitudinal carbon fiber reinforced polymer (CFRP) bars and without vertical shear reinforcement. All beams were tested under a two-point loading system to investigate shear behavior of CFRP reinforced concrete beams. Beam depth and amount of CFRP reinforcement were the main parameters investigated. All beams failed due to a sudden diagonal shear crack at almost 45°. A simplified, empirical expression for the shear capacity of FRP reinforced concrete members accounting for most influential parameters is developed based on the design-by-testing approach using a large database of 134 specimens collected from the literature including the beams tested in this study. The equations of six existing design standards for shear capacity of FRP reinforced concrete beams have also been evaluated using the large database collected. The existing shear design methods for FRP reinforced concrete beams give either conservative or unsafe predictions for many specimens in the database and their accuracy are mostly dependent on the effective depth and type of FRP reinforcement. On the other hand, the proposed equation provides reasonably accurate shear capacity predictions for a wide range of FRP reinforced concrete beams.

Key words: A: Concrete; A: Fiber reinforced polymers; B: Shear strength.

NOMENCLATURE

a	=	beam shear span.
A_{fl}	=	area of longitudinal FRP reinforcement.
a/d	=	beam shear span to effective depth ratio.
b_w	=	beam width.
b_l	=	least-square fine-tuning parameter.
C_1, C_2, C_3 and C_4	=	constants required to model size effect.
CoV	=	coefficient of variation of the error random variable δ .
d	=	beam effective depth.
E_c	=	modulus of elasticity of concrete.
E_{fl}	=	modulus of elasticity of FRP reinforcement.
E_s	=	modulus of elasticity of steel.
f_c'	=	compressive strength of concrete.
f_{cu}	=	cube compressive strength of concrete ($\cong 1.25 f_c'$).
f_{fu}	=	tensile rupture of FRP bars.
f_t	=	tensile strength of concrete.
h	=	overall depth of beams.
M_f	=	bending moment at critical section considered.
n	=	total number of test specimens.
n_f	=	E_{fl} / E_c = ratio of modulus of elasticity of FRP bars to that of concrete.
P	=	total failure load.
P_{cr}	=	total load at first visual crack.
V_c	=	shear capacity provided by concrete reinforced with longitudinal steel bars.
V_{cf}	=	shear capacity provided by concrete reinforced with longitudinal FRP bars.
V_{exp}	=	experimental shear capacity of database specimens.
V_f	=	shear force at critical section considered.
V_{fv}	=	shear capacity provided by FRP stirrups.
V_{pred}	=	predicted shear capacity of database specimens.
δ	=	error random variable.
$\bar{\delta}$	=	mean value of error random variable δ .
σ	=	standard deviation of error random variable δ .
λ	=	factor to account for concrete density (=1.0 in this study).
ρ	=	tensile steel reinforcement ratio.
ρ_{fl}	=	tensile FRP reinforcement ratio.
τ_{rd}	=	design shear stress.

1. INTRODUCTION

Fiber reinforced polymer (FRP) bars are recently used as an alternative to steel reinforcement to overcome corrosion of steel reinforced concrete structures in severe environment. The mechanical properties of FRP are different from these of steel; however, they are dependent on the type and amount of fibre and resin used. Generally, FRP has lower weight and modulus of elasticity but higher strength than steel. In addition, FRP stress-strain curve is straight up to failure, exhibiting a brittle nature.

Most of the current shear design provisions [1-6] follow the well-known $V_{cf} + V_f$ approach to compute the shear resistance of FRP reinforced concrete members, where V_{cf} and V_f are the concrete and FRP stirrup contributions to the shear resistance, respectively. The concrete contribution V_{cf} to shear resistance consists of several shear transfer mechanisms, namely shear resistance of un-cracked concrete in compression zone, aggregate interlock along shear cracks and dowel action of longitudinal reinforcement. Due to the lower elastic modulus and axial rigidity of FRP flexural reinforcement than steel, concrete members reinforced longitudinally with FRP bars develop wider and deeper cracks, and smaller un-cracked concrete compression zone than these reinforced with steel, consequently a reduction in the contributions of un-cracked concrete and aggregate interlock mechanisms to the concrete shear strength. Additionally, due to the relatively small transverse strength of FRP bars and wider cracks, the contribution of dowel action to shear capacity can be very small compared with that of steel. Therefore, concrete members reinforced longitudinally with FRP bars experience reduced shear strength compared with these reinforced with the same amount of steel reinforcement as evidenced in many experimental investigations [7-9].

Many research investigations on the shear strength of reinforced concrete [10-16] indicated that as the beam depth increases, there is a decrease in the shear strength of the member; that has been often termed as 'size effect'. ACI Committee 445 [10] on shear and torsion

suggested that size effect is mainly attributed to the large width of diagonal cracks in larger reinforced concrete beams. Contrasting theories on sound physical modeling of the size effect phenomenon are being debated, primarily the energetic-statistical scaling [13-15] and the crack spacing hypothesis incorporated in the modified compression field theory [11, 12, 16]. Size effect is also of fundamental and practical relevance to the design of concrete members reinforced with FRP bars, where deeper and wider cracks due to the relatively low elastic modulus as well as the reduced dowel action contributed by FRP flexural reinforcement, pose safety concerns that must be addressed.

Although the number of experimental studies on shear behavior of FRP reinforced concrete beams has increased in recent decades, it is still far much lower than that related to steel reinforced concrete structures. On the other hand, several shear design guidelines [1-6] have been published to aid the design of FRP reinforced concrete beams. Most of these design standards consider the size effect in their shear equations in a similar way to conventional steel reinforced concrete but calibrated against limited experimental results. Therefore, it is important to assess the accuracy of these equations against more experimental results. Furthermore, it would be beneficial to propose shear capacity equation accounting for size effect as well as other influential parameters, that accurately predicts the shear capacity of FRP reinforced concrete beams.

The principal objectives of this paper are summarized below:

- To present results of six concrete beams reinforced with CFRP bars tested under static loading condition up to shear failure. Different arrangements of longitudinal CFRP bars and beam depths were investigated.
- To assess the recently developed guideline formulas for estimating the shear capacity of FRP reinforced concrete beams on a large database.

- To propose a shear capacity equation for FRP reinforced concrete beams accounting for size effect as well as other shear design parameters, developed from the well-known design-by-testing approach.

2. TEST PROGRAMME

2.1 Test specimens

The test specimens consisted of six CFRP reinforced concrete beams, classified into three groups according to the overall beam depth. All beams were 200mm wide and 3000mm long. The overall depths of beams in groups 1, 2 and 3 were 400, 300 and 200mm, respectively as given in Table 1 and Fig. 1. In each group, one beam was reinforced with two main longitudinal CFRP bars and the other with four main longitudinal CFRP bars, each of 7.5mm diameter and having 20mm cover concrete. The shear span to effective depth ratios, a/d , for beams in groups 1, 2 and 3 were 2.7, 3.6 and 5.9, respectively as given in Table 1. Beam notations included two parts: the first part gives the overall beam depth (400, 300 or 200mm) and the second part represents the number of main longitudinal bottom CFRP bars (2 or 4 bars). For example, B-300-2 indicates a 300mm deep beam reinforced with 2 CFRP bottom longitudinal bars.

2.2 Material Properties

All test specimens were made from a commercial ready-mixed concrete. Table 1 gives the compressive and tensile strengths of concrete. The concrete compressive strength f_{cu} is obtained from testing sixteen 100 mm cubes whereas the tensile strength f_t of concrete is obtained from the splitting cylinder test of eight cylinders (150mm diameter x 300 mm long), for each series.

The CFRP bars used in this study are manufactured by the pultrusion process. The mechanical properties of CFRP bars used were obtained by carrying out uni-axial tensile tests on three CFRP specimens. Special arrangement for the bar end gripping has to be taken to avoid

crushing of CFRP specimens at the steel jaws of the test machine. CFRP bar specimens were initially prepared by embedding the ends of the CFRP bar into steel tubes filled with a mortar matrix made from high strength gypsum cement. The measured tensile rupture f_{fu} and elastic modulus E_{ft} for 7.5mm diameter CFRP bars were 1100 N/mm^2 and 141440 N/mm^2 , respectively.

3. TEST RESULTS AND DISCUSSIONS

All test specimens, each of 2800 mm span, were simply supported and subjected to a symmetrical two-point loading system as depicted in Fig. 1. A top steel spreader beam was used to divide the total applied load from the hydraulic pump unit into two equal point loads. The load was applied in small increments until failure occurred.

3.1 Failure modes and loads

The first visual crack occurred close to the beam mid-span in the vertical direction at different load levels depending on the amount of CFRP reinforcement used and beam depth as given in Table 1. As the load increased, more flexural cracks were formed within the mid-span and shear span regions and existing cracks became wider and deeper as shown in Fig. 2. Some flexural cracks extended almost across the whole beam depth due to the low elastic modulus to tensile strength ratio of CFRP bars.

All beams failed due to diagonal shear cracks formed within the shear span of test specimens at different load levels as presented in Table 1. Shear failure cracks followed the principal tensile stress trajectories of elastic analysis. At the middle portion of the beam shear span, cracks were almost diagonal at 45° inclination, whereas those at the top-side of the beam were flatter as shown in Fig. 3(a) for beam B-400-2. In beams B-300-2, B-300-4, B-200-2 and B-200-4, the diagonal failure crack propagated horizontally at the level of CFRP bars, showing

signs of debonding between CFRP bars and concrete as depicted in Fig. 3(b) for beam B-300-4.

The amount of longitudinal *bottom* CFRP reinforcement had no significant effect on the shear capacity of beams tested; for example the shear capacity increase in series 1 is 9.8% (beams B-400-2 and B-400-4), series 2 is 0% (beams B-300-2 and B-300-4) and series 3 is 18% (beams B-200-2 and B-200-4). This observation agrees well with that found by Yost et al. [8] for GFRP reinforced concrete beams of similar shear span to depth ratios.

4. EVALUATION OF EXISTING SHEAR DESIGN GUIDELINES

4.1 Review of current shear design provisions

Shear design equations for FRP reinforced concrete members without stirrups recommended by ACI 440.1R-06 [1], CAN/CSA S806-02 [2], JSCE-97 [4], ISIS-M03-07 [3], BISE-99 [5] and CNR-DT 203/2006 [6] listed in Table 2 are evaluated in this study. Note that all strength reduction design factors are set equal to one in these shear design equations for comparison purposes.

Most of the current shear design provisions for concrete structures reinforced with FRP bars are mainly based on the design formulas for concrete members reinforced with steel and modified to account for the difference between FRP and steel reinforcements. Nevertheless, the concrete contribution V_{cf} is different in the manner that it has been calculated in these guidelines. For example, the Japan Society of Civil Engineers (JSCE-97) [4], the British Institution of Structural Engineers guidelines (BISE-99) [5], the Italian Research Council (CNR-DT 203/2006) [6] and the ISIS Canada design manual (ISIS-M03-07) [3] apply a correction factor E_{fl}/E_s that takes into account the difference in the elastic modulus of FRP, E_{fl} , and steel reinforcement, E_s . However, this modification factor E_{fl}/E_s is raised to different powers in these guidelines. On the other hand, the modification proposed by the American

Concrete Institute design guide (ACI 440.1R-06) [1] and the Canadian Standards Association (CAN/CSA S806- 02) [2] only includes the FRP reinforcement axial rigidity $E_{fl} A_{fl}$. However, CAN/CSA S806- 02 ignores the effect of FRP reinforcement axial rigidity for members having an effective depth greater than 300mm that could cause discrepancy in shear capacity prediction close to an effective depth equal to 300mm.

4.2 Size effect modelling in codes

It has been known for many years that shear strength of concrete members without stirrups shows size effect, i.e. nominal shear stress at failure decreases as the member depth increases. Size effect has been modelled in various codes presented in Table 2 using a purely empirical methodology. Some codes use a fractional form, $\frac{C_1}{C_2 + d}$, of the effective depth d for size effect, where C_1 and C_2 are two constants, such as in CAN/CSA S806-02 and ISIS M03-07. It is worth noting that CAN/CSA S806-02 and ISIS M03-07 formulas for members with effective depth greater than 300mm are the same when $\sqrt{E_{fl} / E_s} = 0.5$, that is the case of $E_{fl} = 50$ GPa and $E_s = 200$ GPa. JSCE-97 and BISE-99 have adopted a power series form, $(C_3 / d)^{C_4}$, of the effective depth d for the size effect, where C_3 and C_4 are two constants; C_4 has the same value of 0.25 in both codes as presented in Table 2. CNR-DT 203/2006 formula developed from an old version of Eurocode 2 for the shear capacity of concrete reinforced with steel used a linear reduction form, $1.6 - d \geq 1$, of the effective depth d for the size effect. Generally, various constants required for the size effect modelling are obtained by calibration against limited experimental results. On the other hand, ACI 440.1R-06 does not consider any size effect in the shear capacity prediction formula.

Figure 4 presents the size effect parameters in the five codes of practice against the effective depth d of FRP reinforced concrete members. In Fig. 4, the size effect in CAN/CSA S806-02

is assumed to be the same as that in ISIS M03-07. The trend in each model agrees with the common knowledge of the size effect as the member depth increases, the concrete shear strength decreases. However, the CNR-DT 203/2006 size effect model does not show any reduction when d is greater than 600mm. The values of the size effect parameters proposed by CNR-DT 203/2006, JSCE-97 and BISE-99 are far much larger (around four to five times larger) than these by CAN/CSA S806-02 and ISIS M03-07.

4.3 Experimental database

In addition to the six new test results from the current investigation, the shear strength results of 128 FRP reinforced concrete elements without stirrups were collected from published literature [7-9, 17-34] to evaluate the current shear design guidelines and calibrate the proposed equation in this study. Only rectangular, simply supported beams and slabs that exhibited shear failure were considered. All specimens were tested under a two-point loading system, and had a shear span-to-depth ratio, a/d , larger than 2.5. The database specimens included 126 beams and 8 one-way slabs of which 6 were reinforced with aramid FRP (AFRP) bars, 51 with CFRP bars and 77 with glass FRP (GFRP) bars. Table 3 gives the distribution of the main shear design parameters in the database. Very few shear tests (only 4) have been conducted on specimens having an effective depth greater than 400mm as indicated from the distribution in Table 3. Each shear design method was evaluated based on both the ratio of experimental to predicted shear capacities, V_{exp}/V_{pred} , and the average absolute error (AAE) calculated from:

$$AAE = \frac{1}{n} \sum \frac{|V_{exp} - V_{pred}|}{V_{exp}} \times 100 \quad (1)$$

where n is the total number of test specimens.

4.4 Proposed shear equation

The equation developed by Zsutty [35] is one of the simplest and reliable empirical shear equation for steel reinforced concrete beams without stirrups. This equation, in SI units, includes the effect of the shear span to depth ratio and reinforcement ratio as follows:

$$V_{cs} = 2.2 \left(\rho \frac{d}{a} f'_c \right)^{1/3} b_w d \quad (2)$$

where V_{cs} is the shear capacity (in N) of concrete elements reinforced with steel and ρ is the tensile steel reinforcement ratio and other parameters are the same as defined earlier. In the present study, a theoretical model for the shear resistance $V_{cf,the}$ of FRP elements based on Eq. (2) but modified to account for the axial rigidity of FRP longitudinal reinforcement and to consider the size effect is proposed below:

$$\begin{aligned} V_{cf,the} &= 2.2 \left(r_{fl} \frac{E_{fl}}{E_s} \frac{d}{a} f'_c \right)^{1/3} b_w d & d \leq 300 \text{ mm} \\ V_{cf,the} &= 2.2 \left(r_{fl} \frac{E_{fl}}{E_s} \frac{d}{a} f'_c \right)^{1/3} \left(\frac{300}{d} \right)^{0.25} b_w d & d > 300 \text{ mm} \end{aligned} \quad (3)$$

The size effect parameter $(300/d)^{0.25}$ is similar to the one proposed in BISE-99 but considered only for elements having $d > 300$. The main feature of Eq. (3) is that it accounts for size effect as well as other design parameters affecting the shear capacity of FRP reinforced concrete beams.

The above theoretical shear resistance model will be fine-tuned using the design-by-testing approach proposed in Annex D of EN 1990 [36] and successfully employed to develop models for the intermediate and end de-bonding failure of externally bonded fibre reinforced polymer sheets to steel reinforced concrete beams [37, 38, 39]. The main aim of the design-by-testing approach is to develop a formula for characteristic or design shear resistance from the mean shear resistance (Eq. 3 above) using experimental results.

The shear resistance V_{cf} is, therefore, represented in the following probabilistic model form:

$$V_{cf} = b_1 V_{cf,the} \delta \quad (4)$$

where b_1 is a least-square fine-tuning parameter, given by $b_1 = \sum V_{exp} V_{cf,the} / \sum V_{cf,the}^2$, and δ is an error random variable obtained from a comparison of the experimental shear capacity and corrected theoretical shear resistance for each specimen in the database, i.e.,

$$\delta_i = \frac{(V_{exp})_i}{(c_1 V_{cf,the})_i} \quad (5)$$

where $i = 1$ to 134. The least-square fine-tuning parameter b_1 obtained from 134 database is 1.255 and, therefore, the mean shear resistance V_{cf} can be calculated from:

$$\begin{aligned} V_{cf,the} &= 2.76 \left(r_{fl} \frac{E_{fl}}{E_s} \frac{d}{a} f'_c \right)^{1/3} b_w d & d \leq 300mm \\ V_{cf,the} &= 2.76 \left(r_{fl} \frac{E_{fl}}{E_s} \frac{d}{a} f'_c \right)^{1/3} \left(\frac{300}{d} \right)^{0.25} b_w d & d > 300mm \end{aligned} \quad (6)$$

Fig. 5 shows the comparisons between the shear resistance obtained from Eq. 6 and the experimental results of all 134 test specimens. The mean value, $\bar{\delta}$, standard deviation, σ , and coefficient of variation, CoV , of the error random variable δ can be calculated from:

$$\bar{\delta} = \frac{1}{n} \sum_{i=1}^n \delta_i, \quad \sigma = \sqrt{\frac{1}{n-1} \sum_{i=1}^n (\delta_i - \bar{\delta})^2}, \quad CoV = \sigma / \bar{\delta} \quad (7)$$

The above values for δ considering the comparison with the 134 test specimens are $\bar{\delta} = 1.002$, $\sigma = 0.252$ and $CoV = 0.251$, indicating the high level of accuracy of Eq. (7). These statistical values of δ are also particularly important for defining the 5% percentile of the shear resistance defined in Eq. (4).

Figure 6 compares the cumulative distribution of the error random variable δ against the theoretical Gaussian distribution having the same mean value and standard deviation. It shows that the cumulative distribution of δ is very similar to the standard normal distribution curve,

validating the normality hypothesis of error. Therefore, the characteristic value, $V_{cf,k}$, of shear resistance V_{cf} can be calculated from:

$$V_{cf,k} = V_{cf,m} - 1.64\sqrt{\text{Var}(V_{cf})} \quad (8)$$

As the basic random variables, E_{fl} , ρ_{fl} , a , d , b_w , and f'_c required by Eq. (4) can be considered as statistically independent variables, the variance $\text{Var}(V_{cf})$ can be calculated from:

$$\text{Var}(V_{cf}) = \sum [k_i^2 x \text{Var}(x_i)] + k_\delta^2 x \text{Var}(\delta) \quad (9)$$

where k_i and k_δ are the values of the partial derivatives of V_{cf} with respect to the basic variables x_i and the error variable δ calculated at the mean values of x_i and δ .

The basic random variables can also be divided into two categories; namely the geometrical parameters (a , d , b_w and ρ_{fl}) and material properties (E_{fl} and f'_c). Assuming the parameters related to the member geometry are deterministic variables with zero variation and the material properties related variables are normally distributed random variables, Eq. 9 above may be written as below:

$$\text{Var}(V_{cf}) = \left(\frac{\partial V_{cf}}{\partial E_{fl}} \right)^2 \text{Var}(E_{fl}) + \left(\frac{\partial V_{cf}}{\partial f'_c} \right)^2 \text{Var}(f'_c) + \left(\frac{\partial V_{cf}}{\partial \delta} \right)^2 \text{Var}(\delta) \quad (10)$$

where $\frac{\partial V_{cf}}{\partial E_{fl}} = \frac{V_{cf}}{3E_{fl}}$, $\frac{\partial V_{cf}}{\partial f'_c} = \frac{V_{cf}}{3f'_c}$, $\frac{\partial V_{cf}}{\partial \delta} = V_{cf}$

The characteristic shear resistance $V_{cf,k}$ can be, then, obtained from:

$$V_{cf,k} = V_{cf,m} \left(1 - 1.64 \left(\frac{\text{Var}(E_{fl})}{9E_{fl}^2} + \frac{\text{Var}(f'_c)}{9(f'_c)^2} + \text{Var}(\delta) \right)^{\frac{1}{2}} \right) \quad (11)$$

As the number of specimens used in each experimental investigation collected from the literature were very small to allow the calculations of the coefficient of variations for the

variables f'_c and E_{ft} , nominal values of CoV for E_{ft} and f'_c may be reasonably assumed as [37,40]:

$$\text{CoV for } f'_c = 4.88 / f'_c \quad \text{CoV for } E_{ft} = 0.05 \quad (12)$$

However, the coefficient of variation of δ is obtained from the statistical distribution of the comparison between the theoretical and 134 experimental shear capacities as obtained above (CoV=0.251).

4.5 Theoretical prediction of shear capacity

Figure 7 shows a comparison between experimental and predicted shear capacities $V_{\text{exp}}/V_{\text{pred}}$ obtained from the proposed and current design equations for the database test specimens. The vertical axis in this figure represents the ratio $V_{\text{exp}}/V_{\text{pred}}$, while the horizontal axis is the effective depth d of FRP reinforced concrete members. The mean, standard deviation (SD) and coefficient of variation (COV) for $V_{\text{exp}}/V_{\text{pred}}$, and AAE of all design shear equations are also listed in Table 4.

Table 4 and Fig. 7(a) show that the ACI 440.1R-06 design method provides the most conservative predictions and scatter with all predictions in the conservative side and mean ratio of $V_{\text{exp}}/V_{\text{pred}}$ of 1.89, even though the safety factor was not considered. This relatively high level of conservatism could be attributed to the fact that the ACI 440.1R-06 method considers the concrete shear strength to be provided only by the uncracked concrete above the neutral axis [41]. On the other hand, the proposed equation provides the most reasonable prediction and least scatter for shear strength of FRP reinforced concrete beams with an average ratio of $V_{\text{exp}}/V_{\text{pred}}$ equal to 1.00. The proposed equation also provided the lowest AAE of 16.6% compared with 43.8% for ACI 440.1R-06, 33% for ISIS-M03-07, 28.8% for CNR-DT, 24.8% for JSCE-97, 23.7% for CAN/CSA S806-02 and 18.6% for BISE-99.

A further statistical analysis has been performed separating members in the database based on their effective depth d and type of longitudinal FRP reinforcement used. Table 5 presents the mean, standard deviation and coefficient of variation for members having $d \leq 300\text{mm}$ and $d > 300\text{mm}$ and those reinforced with CFRP, AFRP and GFRP bars. Since AFRP has a similar modulus of elasticity to GFRP and the number of specimens reinforced with AFRP bars in the database is not large enough to give meaningful statistical parameters, specimens reinforced with GFRP or AFRP are combined together in one group in this section of the paper. Figure 8 also presents the mean ratio of $V_{\text{exp}}/V_{\text{pred}}$ for different categories as predicted by each method. Overall, the predictions obtained from each method vary considerably among the four different cases considered. The CAN/CSA S806-02 design method shows the largest inconsistency with a mean of $V_{\text{exp}}/V_{\text{pred}}$ for CFRP specimens having $d > 300\text{mm}$ of 2.12 and that for CFRP specimens having $d \leq 300\text{mm}$ of 1.14. For all methods considered, the highest and lowest mean ratios of $V_{\text{exp}}/V_{\text{pred}}$ were always for CFRP reinforced concrete specimens having $d > 300\text{mm}$ and $d \leq 300\text{mm}$, respectively. CNR-DT 203/2006 predictions are un-conservative for many specimens, especially those reinforced with CFRP bars and having $d \leq 300\text{mm}$ as shown in Fig. 8 and reflected in the mean of the ratio $V_{\text{exp}}/V_{\text{pred}}$ of 0.66. ISIS M03-07 was also un-conservative in predicting the shear capacity of CFRP reinforced concrete specimens having $d \leq 300\text{mm}$. Analysis of the database indicated that most of these beams for which ISIS-M03-07 overestimated the shear capacity had shear-span to effective depth ratios (a/d) greater than 3. This could be attributed to the fact that ISIS-M03-07 method does not consider the contribution of some shear design parameters such as the longitudinal FRP reinforcement ratio, ρ_{fl} , and the shear span to depth ratio, a/d . On the other hand, CAN/CSA S806-02 shear design equation highly underestimated the shear capacity of CFRP reinforced concrete specimens with $d > 300\text{mm}$ (mean of $V_{\text{exp}}/V_{\text{pred}}=2.12$) as it considers a constant value of $E_f=50$ GPa for all types of FRP bars [9] in specimens having $d > 300\text{mm}$.

This value is close to E_f for GFRP and AFRP, but much lower than that of CFRP, leading to a lower-bound for concrete contribution to shear capacity of CFRP reinforced concrete members.

Shear design provision of JSCE-97 gives conservative predictions for FRP reinforced concrete beams having $d > 300$ mm. Similar observations are also valid, to a less extent, for the shear equation proposed by BISE-99. However, JSCE-97 and BISE-99 methods provide reasonable estimations for the shear capacity of FRP reinforced concrete beams with $d < 300$ mm.

Overall, Table 5 and Fig. 8 shows that the accuracy of existing shear design equations vary with the member effective depth and type FRP reinforcement. On the other hand, as observed from Tables 4 and 5, and Figs. 7(g) and 8, the proposed design equation provides reasonably accurate predictions for a wide range of specimens regardless of the beam size and type of FRP reinforcement.

5. CONCLUSIONS

Test results of six CFRP reinforced concrete beams have been presented. A simplified, empirical equation accounting for size effect as well as all other shear design parameters was developed based on the well-known design-by-testing approach using a large database of 134 test specimens collected from the literature including the beams tested in this study. Six existing shear design methods have also been evaluated using the large database collected. Based on the above investigation, the following conclusions may be drawn:

- The failure of all beams tested was due to 45° diagonal shear cracks.
- The amount of longitudinal bottom CFRP reinforcement had no significant effect on the shear capacity of beams tested.

- The ACI 440.1R-06 shear design method provided the most conservative predictions and scatter with all predictions in the conservative side, even though the safety factor was not considered.
- The values of size effect parameter proposed by CNR-DT 203/2006, JSCE-97 and BISE-99 are far much higher than these in CAN/CSA S806-02 and ISIS M03-07.
- CNR-DT 203/2006 predictions are highly un-conservative for many specimens, especially those reinforced with CFRP and having an effective depth less than 300mm.
- The accuracy levels of existing shear design equations vary considerably with different cases considered for the effective depth and type of FRP reinforcement. CAN/CSA S806-02 method exhibited the widest variation in predicting the shear capacity of concrete elements reinforced with different types of FRP and having an effective depth larger or smaller than 300mm.
- The shear capacity prediction for CFRP reinforced concrete specimens with an effective depth greater than 300mm was highly underestimated and that for CFRP reinforced concrete specimens having an effective depth less than 300mm was generally un-conservative by most codes considered.
- The simplified proposed equation gives reasonably accurate predictions for a wide range of specimens regardless of beam size and type of FRP reinforcement.

6. REFERENCES

- [1] American Concrete Institute (ACI), “Guide for the design and construction of concrete reinforced with FRP bars”, Technical Committee Document No. 440.1R-06, Farmington Hills, Mich. (2006).

- [2] Canadian Standards Associations (CSA), “Design and construction of building components with fibre-reinforced polymers”, Canadian Standards S806-02, Rexdale, Ontario, Canada, (2002).
- [3] ISIS Canada, “Reinforcing concrete structures with fiber reinforced polymers”, ISIS-M03-07, Canadian Network of Centers of Excellence on Intelligent Sensing for Innovative Structures, Univ. of Winnipeg, Winnipeg, Man, (2007).
- [4] Japan Society of Civil Engineers (JSCE), “Recommendations for design and construction of concrete structures using continuous fibre reinforced materials”, Concrete Engineering Series 23, A. Machida, ed, Tokyo, Japan, (1997).
- [5] British Institution of Structural Engineers (BISE), “Interim guidance on the design of reinforced concrete structures using fiber composite reinforcement”, *IStructE*, SETO Ltd., London, (1999)
- [6] CNR-DT 203/2006, “Guide for the design and construction of concrete structures reinforced with fiber-reinforced polymer bars”, National Research Council, Rome, Italy, (2006).
- [7] S. Tottori, H. Wakui, “Shear capacity of RC and PC beams using FRP reinforcement”, In: Fiber-reinforced-plastic reinforcement for concrete structures, SP-138. Detroit: American Concrete Institute, 615–632, (1993)
- [8] J.R. Yost, S.P. Gross, D.W. Dinehar, “Shear strength of normal strength concrete beams reinforced with deformed GFRP bars”, *J. Compos. Construct.*, 5(4):268–75, (2001).
- [9] A.K. El-Sayed, E.F. El-Salakawy, B. Benmokrane, “Shear Strength of FRP-Reinforced Concrete Beams without Transverse Reinforcement”, *ACI Struct. J.*, 103(2), 235-243, (2006).
- [10] Joint ACI Committee 445. Recent approach to shear design of structural concrete, *J Struct Engrg*, 1995, 1375-1417.

- [11] Lubell A, Sherwodd, T, Bentz EC, Collins MP. Safe shear design of large wide beams. *Concr Int*, 2004; 26(1), 66-78.
- [12] Reineck, KH. Ultimate shear force of structural concrete members without transverse reinforcement derived from a mechanical model. *ACI Struct J*, 1991; 88(5), 592-602.
- [13] Bazant, ZP, Kazemi ZP. Size effect on diagonal shear failure of beams without stirrups. *ACI Struct J*, 1991; 88(3), 268-276.
- [14] Bazant, ZP, Kim JK. Size effect in shear failure of longitudinally reinforced beams. *ACI Struct J*; 1984, 81(5), 456- 468
- [15] Bazant ZP, Yu Q. Designing against size effect on strength of reinforced concrete beams without stirrups: I. Formulation. *J of Struct. Engrg.*, 2005 131(12), 1877-1885.
- [16] Collins MP, Mitchell D, Adebar P, Vecchio FJ. A general shear design method. *ACI Struct J*; 1996, 93(1), 36-45.
- [17] A.F. Ashour, “Flexural and shear capacities of concrete beams reinforced with GFPR bars”, *Constr. Build. Mater.*, 20, 1005-1015, (2006).
- [18] A.K. El-Sayed, E.F. El-Salakawy, B. Benmokrane, “Shear Capacity of High-Strength Concrete Beams Reinforced with FRP Bars”, *ACI Struct. J.*, 103(3), 383-389, (2006).
- [19] S.P. Gross, D.W. Dinehart, J.R Yost, P.M Theisz, “Experimental Tests of High-Strength Concrete Beams Reinforced with CFRP Bars”, *Proceedings of the 4 th International Conference on Advanced Composite Materials in Bridges and Structures (ACMBS-4)*, Calgary, Alberta, Canada, July 20-23, 8 p., (2004).
- [20] S.P. Gross, J.R. Yost, D.W. Dinehart, E. Svensen, N. Liu, “Shear Strength of Normal and High Strength Concrete Beams Reinforced with GFPR Reinforcing Bars”, *Proc. of the Int. Conference on High Performance Materials in Bridges*, ASCE, 426-437, (2003).

- [21] M. Tariq, J.P. Newhook, “Shear Testing of FRP reinforced Concrete without Transverse Reinforcement”, Proceedings of CSCE 2003-Annual Conference, Moncton, NB, Canada, 10 p., (2003).
- [22] A.K. Tureyen, R.J. Frosch, “Shear Tests of FRP-Reinforced Concrete Beams without Stirrups”, ACI Struct. J., 99(4), 427-434, (2002)
- [23] T. Alkhrdaji, M. Wideman, A. Belarbi, A. Nanni, “Shear Strength of GFRP RC Beams and Slabs”, Proceedings of the International Conference, Composites in Construction-CCC 2001, Porto/Portugal, 409-414, (2001).
- [24] D.H. Deitz, I.E. Harik, H. Gesund, “One-Way Slabs Reinforced with Glass Fiber Reinforced Polymer Reinforcing Bars”, Proceedings of the 4th International Symposium, Fiber Reinforced Polymer Reinforcement for Reinforced Concrete Structures, MI, 279-286, (1999).
- [25] Y. Mizukawa, Y. Sato, T. Ueda, Y. Kakuta, “A Study on Shear Fatigue Behavior of Concrete Beams with FRP Rods”, Proceedings of the Third International Symposium on Non-Metallic (FRP) Reinforcement for Concrete Structures (FRPRCS-3), Japan Concrete Institute, Sapporo, Japan, 2, 309-316, (1997).
- [26] N. Duranovic, K. Pilakoutas, P. Waldron, “Tests on Concrete Beams Reinforced with Glass Fibre Reinforced Plastic Bars”, Proceedings of the Third International Symposium on Non-Metallic (FRP) Reinforcement for Concrete Structures (FRPRCS-3), Japan Concrete Institute, Sapporo, Japan, 2, 479-486, (1997).
- [27] N. Swamy, M. Aburawi, “Structural Implications of Using GFRP Bars as Concrete Reinforcement”, Proceedings of the Third International Symposium on Non-Metallic (FRP) Reinforcement for Concrete Structures (FRPRCS-3), Japan Concrete Institute, Sapporo, Japan, 2, 503-510, (1997).

- [28] W. Zhao, K. Mayama, H. Suzuki, “Shear Behaviour of Concrete Beams Reinforced by FRP Rods as Longitudinal and Shear Reinforcement”, Proceedings of the Second International RILEM Symposium on Non-Metallic (FRP) Reinforcement for Concrete Structures (FRPRCS-2), Ghent, Belgium, 352-359, (1995).
- [29] A.G. Razaqpur, B.O. Isgor, S. Greenaway, A. Selley, “Concrete contribution to the shear resistance of fiber reinforced polymer reinforced concrete members”, *J. Compos. Constr.*, 8(5), 452–460, (2004).
- [30] A.K. El-Sayed, E.F. El-Salakawy, B. Benmokrane, “Shear strength of one way concrete slabs reinforced with FRP composites bars”, *J. Compos. Constr.*, 9(2), 147-157, (2005).
- [31] A. Lubell, T. Sherwrod, E. Bents, M.P. Collins, “Safe shear design of large”, *Wide Beams Concr. Int.*, 26(1): 67-79, (2004)
- [32] T. Nagasaka, H. Fukuyama, M. Tanigaki, “Shear performance of concrete beams reinforced with FRP stirrups”, In: Nanni A, Dolan C, editors. *ACI SP-138*. Detroit, Mich: American Concrete Institute, p. 789–811, (1993).
- [33] H. Nakamura, T. Higai, “Evaluation of shear strength of concrete beams reinforced with FRP”, *Concrete library international. Proc Jpn Soc Civil Eng.*, 26:111–23, (1995).
- [34] F. Matta, A. Nanni, T.M. Hernandez,, B. Benmokrane, “Scaling of strength of FRP reinforced concrete beams without shear reinforcement”, *Fourth international conference on FRP composites in civil engineering (CICE 2008)*, Zurich, Switzerland, 6p, (2008).
- [35] T.C. Zsutty, “Shear strength prediction for separate categories of simple beam tests”, *ACI Struct. J.*,68(2):138–43, (1971).
- [36] European Committee for Standardization. *EN 1990 – Eurocode – basic of structural design*; 2002.

- [37] A. Bilotta, C. Faella, E. Martinelli, E. Nigro, “Design by testing procedure for intermediate debonding in EBR FRP strengthened RC beams”, *Engrg. Struct.*, 46:147-154, (2003).
- [38] G. Monti, S. Alessandri, S. Santini, “Design by testing: A procedure for the statistical determination of capacity models”, *Constr. Build. Mater.*, 23(4), 1487-1494, (2009).
- [39] A. Bilotta, M. Ludovico, E. Nigro, “FRP-to-concrete interface debonding: Experimental calibration of capacity model”, *Compos Part: B Engrg*, 42:1539-1553, (2011).
- [40] European Committee for Standardization. EN 1992-1-1 – Eurocode-2 – design of concrete structures; 2004.
- [41] A.K. Tureyen, R.J. Frosch, “Concrete shear strength: Another perspective”, *ACI Struct. J.*, 100(5): 609–615, (2003).

List of Tables

Table 1 Details of test specimens.

Table 2 Shear design equations for FRP reinforced concrete beams without stirrups.

Table 3 Distribution of shear design parameters included in the database.

Table 4 Statistical coefficients of the proposed and shear design equations.

Table 5 Further statistical analysis of predicted shear capacity.

Table 1 Details of test specimens.

Series	Beam no.	h (mm)	a/d	No. of 7.5mm bottom bars	f_{cu} (N/mm ²)	f_t (N/mm ²)	P_{cr} (kN)	P (kN)
Series 1	B-400-2	400	2.7	2	27.0	2.1	15.64	65.76
	B-400-4			4			28.64	72.23
Series 2	B-300-2	300	3.6	2	35.0	2.7	9.17	65.76
	B-300-4			4			15.64	65.76
Series 3	B-200-2	200	5.9	2	29.0	2.2	4.58	35.17
	B-200-4			4			4.58	41.50

Note: All beams were 3000mm long and 200mm wide; all notations are defined in the Nomenclature section.

Table 2 Shear design equations for FRP reinforced concrete beams without stirrups.

ACI 440.1R-06	$V_{cf} = \frac{2}{5} \sqrt{f_c'} b_w d (\sqrt{2\rho_{fl} n_f + (\rho_{fl} n_f)^2} - \rho_{fl} n_f)$
CAN/CSA S806-02	$V_{cf} = 0.035 \lambda b_w d \left(f_c' \rho_{fl} E_{fl} \frac{V_f d}{M_f} \right)^{1/3} \quad d \leq 300 \text{ mm}$ $\frac{V_f d}{M_f} \leq 1 \quad \text{and} \quad 0.1 \lambda b_w d \sqrt{f_c'} \leq V_{cf} \leq 0.2 \lambda b_w d \sqrt{f_c'}$ $V_{cf} = \frac{130}{1000 + d} \lambda b_w d \sqrt{f_c'} \quad d > 300 \text{ mm}$ $V_{cf} \geq 0.08 \lambda b_w d \sqrt{f_c'}$
ISIS M03-07	$V_{cf} = 0.2 \lambda b_w d \sqrt{f_c' \frac{E_{fl}}{E_s}} \quad d \leq 300 \text{ mm}$ $V_{cf} = \frac{260}{1000 + d} \lambda b_w d \sqrt{f_c' \frac{E_{fl}}{E_s}} \quad d > 300 \text{ mm}$ $V_{cf} \geq 0.1 \lambda b_w d \sqrt{f_c' \frac{E_{fl}}{E_s}}$
JSCE-97	$V_{cf} = \beta_d \beta_p \beta_n f_{vcd} b_w d$ $\beta_p = \sqrt[3]{\frac{100 \rho_{fl} E_{fl}}{E_s}} \leq 1.5$ $\beta_d = \sqrt[4]{\frac{1000}{d}} \leq 1.5$ $\beta_n = 1.0 \text{ (in case of no axial force)}$ $f_{vcd} = 0.2 \sqrt[3]{f_c'} \leq 0.72 \text{ (MPa)}$
CNR-DT 203/2006	$V_{cf} = 1.3 \left(\frac{E_{fl}}{E_s} \right)^{1/2} (\tau_{rd} k_d (1.2 + 40 \rho_{fl}) b_w d)$ $k_d = 1.6 - d \geq 1$ $1.3 \left(\frac{E_{fl}}{E_s} \right)^{1/2} \leq 1$
BISE-99	$V_{cf} = 0.79 \left(100 \rho_{fl} \frac{E_{fl}}{E_s} \right)^{1/3} \left(\frac{400}{d} \right)^{0.25} \left(\frac{f_{cu}}{25} \right)^{1/3} b_w d$ $\frac{400}{d} \leq 1$
Note: all notations are defined in the Nomenclature section.	

Table 3 Distribution of shear design parameters included in the database.

Web width b_w		Effective depth d		Concrete compressive strength f_c		Shear span to depth ratio a/d		Modulus of elasticity E_{fl}		Reinforcement ratio $\rho_{fl} (\%)$	
Range (mm)	Freq.	Range (mm)	Freq.	Range (MPa)	Freq.	Range	Freq.	Range (GPa)	Freq.	Range	Freq.
80-100	3	100-200	34	20-30	17	2.5-3.0	17	20-50	81	0.1-0.75	44
100-200	69	200-300	57	30-40	55	3.0-3.5	44	50-80	5	0.75-1.25	35
200-300	39	300-400	39	40-50	29	3.5-4.0	15	80-110	3	1.25-1.75	27
300-400	5	400-500	0	50-60	5	4.0-4.5	31	110-140	30	1.75-2.25	17
400-500	10	500-600	0	60-70	10	4.5-5.0	1	140-170	12	2.25-2.75	10
500-1000	8	600-1000	4	70-90	18	5.0-6.5	26	170-200	3	2.75-3.25	1

Note: Total number of beams in the database is 128; of these 6 reinforced with AFRP bars, 51 with CFRP bars and 77 with GFRP bars.

Table 4 Statistical coefficients of the proposed and shear design equations.

Method	V_{exp}/V_{pred}			AAE(%)
	Mean	SD	COV (%)	
ACI 440.1R-06	1.89	0.54	28.5	43.8
CAN/CSA-S806-02	1.36	0.5	36.3	23.7
ISIS M03-07	1.3	0.46	35.1	33
JSCE-97	1.39	0.39	28.2	24.8
CNR-DT 203/2006	0.92	0.30	32.6	28.8
BISE-99	1.15	0.36	31.1	18.6
Proposed Eq.	1.00	0.25	25.1	16.6

Table 5 Further statistical analysis of predicted shear capacity.

Method	Statistical Parameters	V_{exp}/V_{pred}			
		GFRP or AFRP		CFRP	
		d ≤ 300mm	d > 300	d ≤ 300mm	d > 300
Number of Specimens		62	24	29	19
ACI 440.1R-06	Mean	1.87	2.04	1.64	2.11
	SD	0.44	0.84	0.31	0.52
	COV (%)	23.2	41.1	18.9	24.7
CAN/CSA 806-02	Mean	1.21	1.42	1.14	2.12
	SD	0.27	0.54	0.22	0.6
	COV (%)	22	37.8	19	28.4
ISIS M03-07	Mean	1.44	1.54	0.82	1.28
	SD	0.37	0.48	0.28	0.35
	COV (%)	26	31	34.8	27.4
JSCE-97	Mean	1.31	1.58	1.2	1.72
	SD	0.27	0.58	0.17	0.41
	COV (%)	20.6	36.7	14.6	24
CNR DT-203/2006	Mean	0.95	1.1	0.66	1.04
	SD	0.25	0.37	0.16	0.27
	COV (%)	26.6	33.5	23.9	26
BISE-99	Mean	1.07	1.32	0.95	1.47
	SD	0.24	0.52	0.21	0.36
	COV (%)	22.1	39.56	22.1	24.4
Proposed Eq.	Mean	0.98	1.04	0.93	1.14
	SD	0.20	0.38	0.15	0.28
	COV (%)	20.8	36.2	15.9	25

List of Figures

Figure 1 Geometrical dimensions and reinforcement details of test specimens.

Figure 2 Crack pattern of B-300-4 at 60kN (91% of the failure load)

Figure 3 Failure modes of beams tested.

Figure 4 Size effect modelling in various codes of practice.

Figure 5 Comparisons between the proposed equation and experimental results.

Figure 6 Cumulative frequency distribution of the model random variable, δ .

Figure 7 Experimental to predicted shear capacities versus effective depth of FRP members.

Fig. 8 Mean of experimental to predicted shear capacities for various categories of specimens in the database.

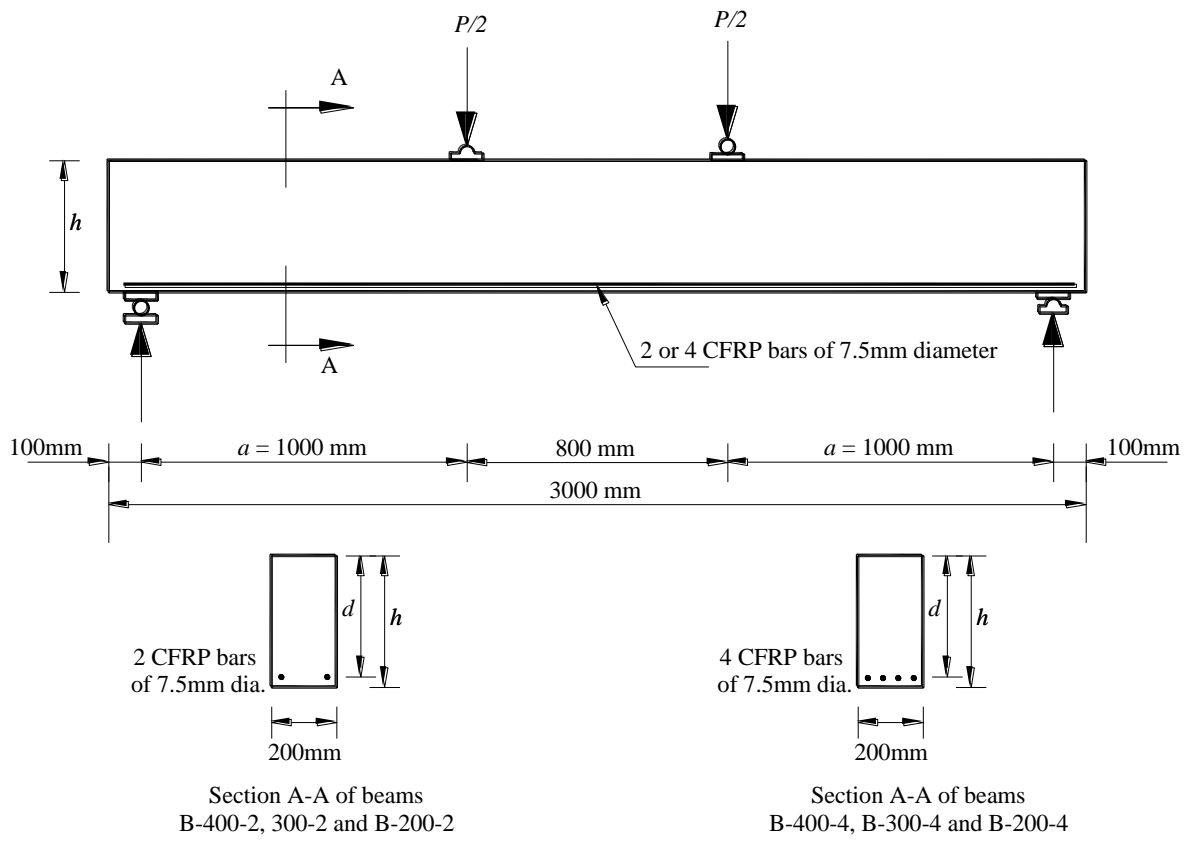


Figure 1 Geometrical dimensions and reinforcement details of test specimens

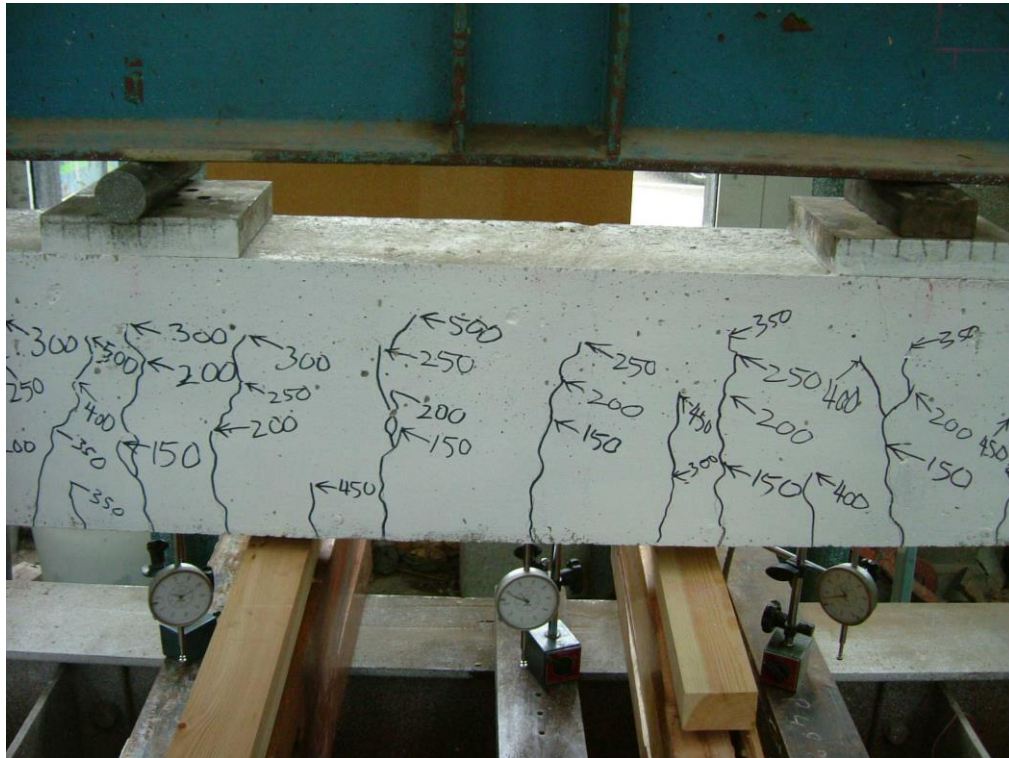
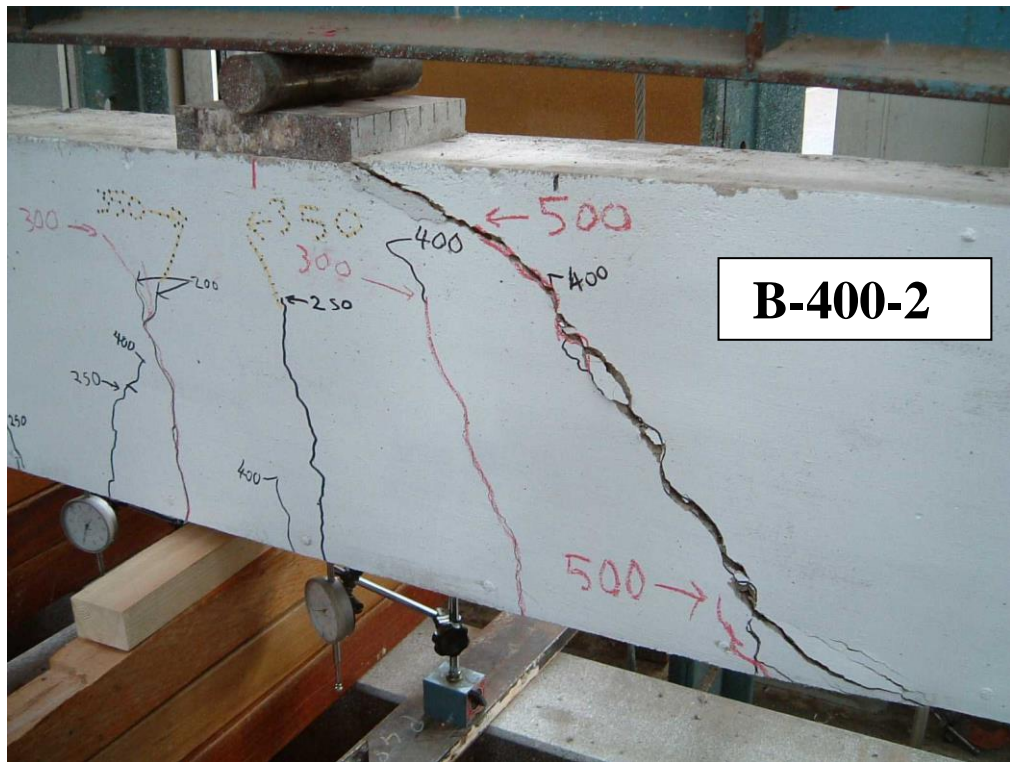
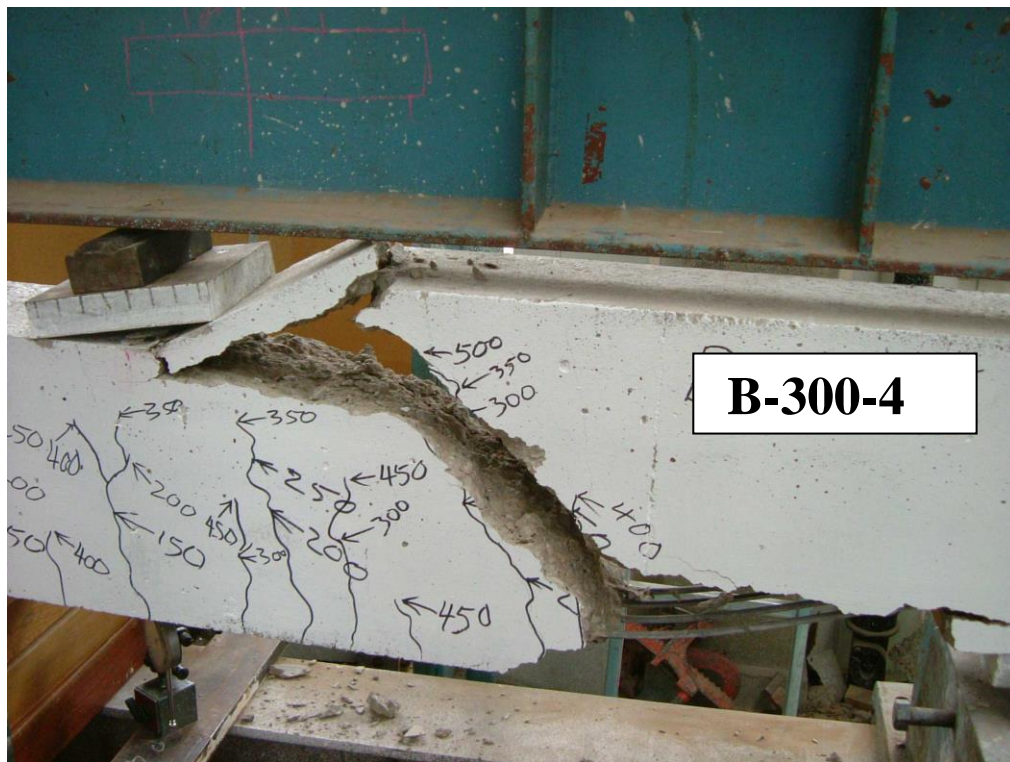


Figure 2 Crack pattern of B-300-4 at 60kN (91% of the failure load)



(a) Diagonal shear crack at failure for Beam B-400-2



(b) Diagonal shear crack and debonding of CFRP bars at failure for Beam B-300-4

Figure 3 Failure modes of beams tested.

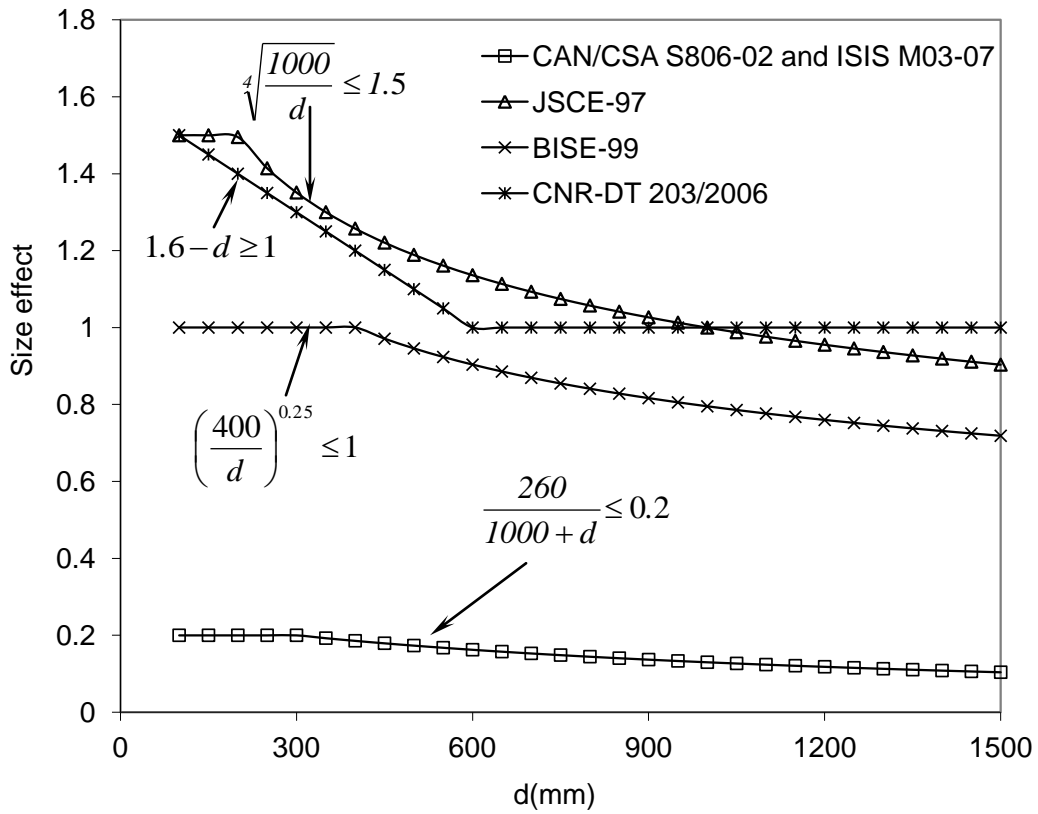


Figure 4 Size effect modelling in various codes of practice.

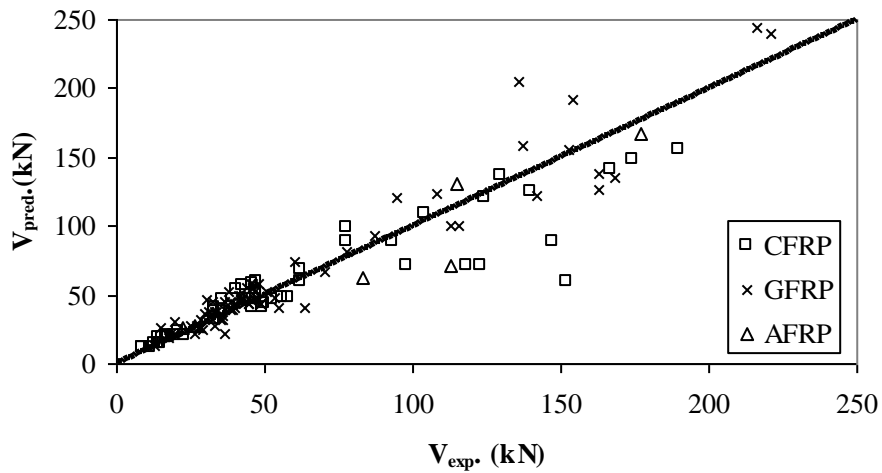


Figure 5 Comparisons between the proposed equation and experimental results.

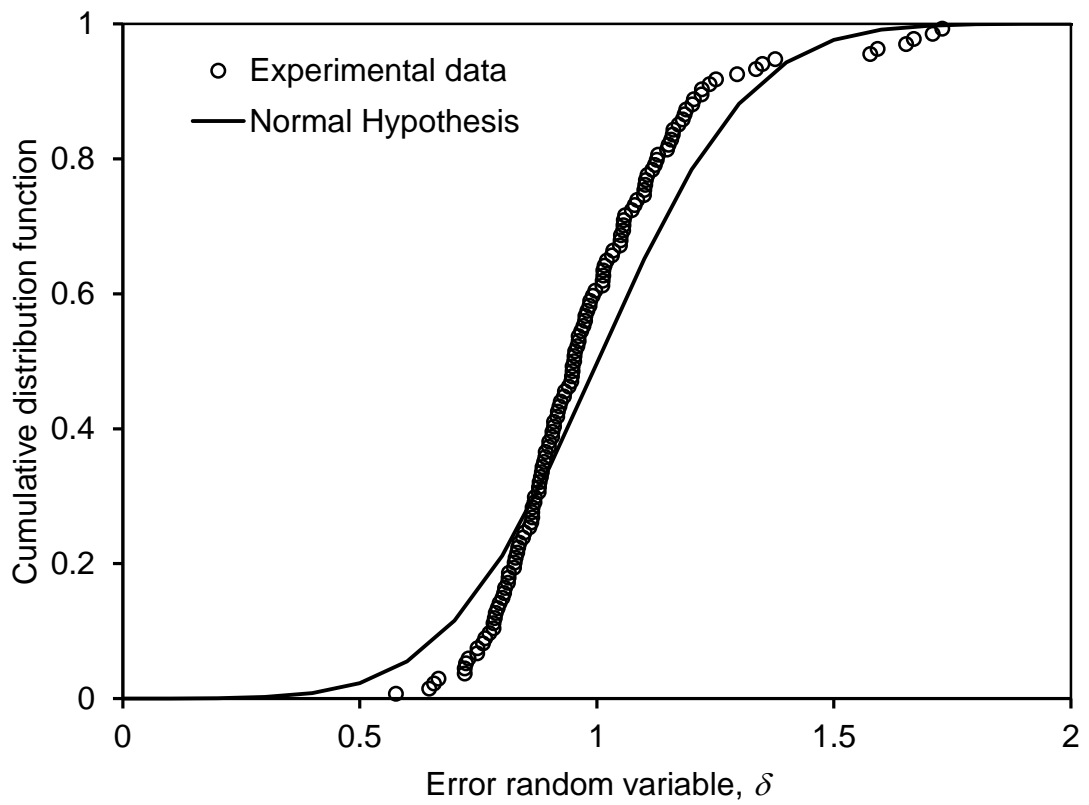
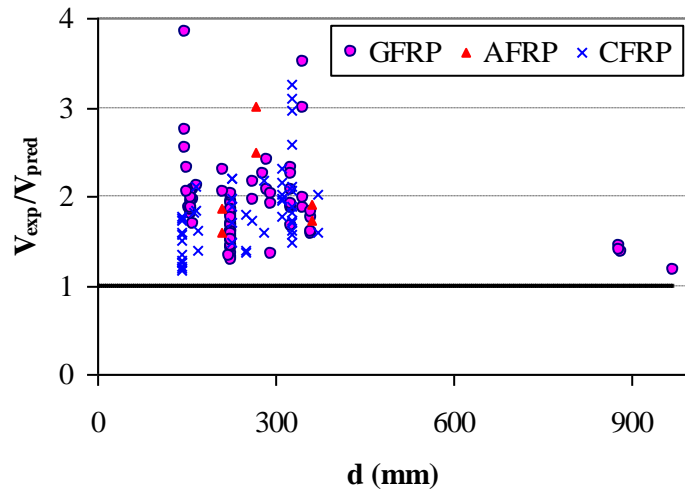
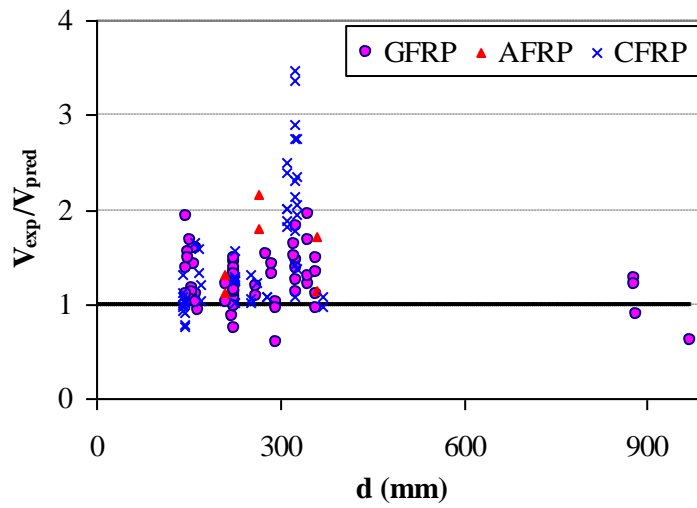


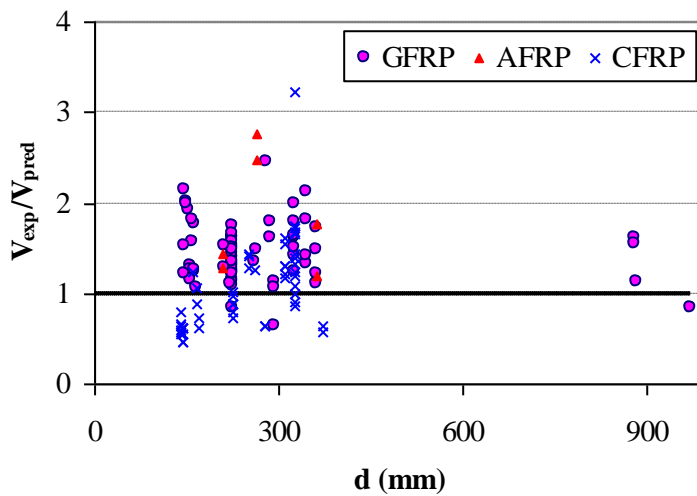
Figure 6 Cumulative frequency distribution of the model random variable, δ .



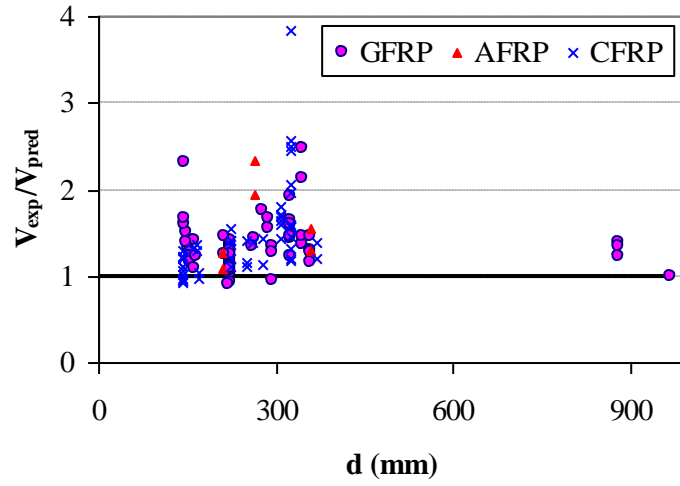
(a) ACI 440-06



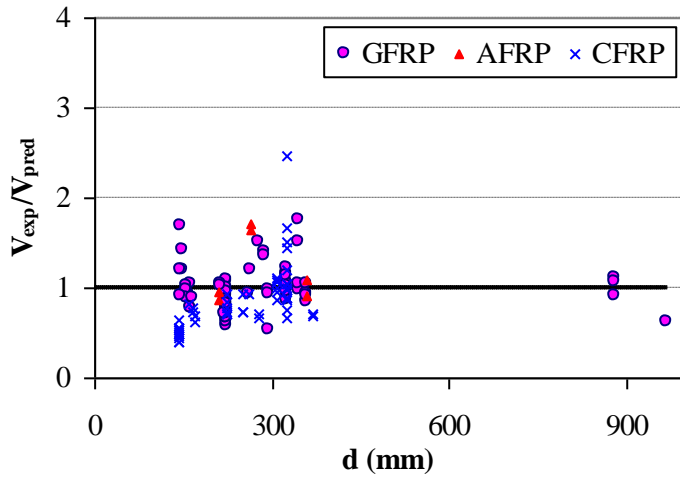
(b) CSA S806-02



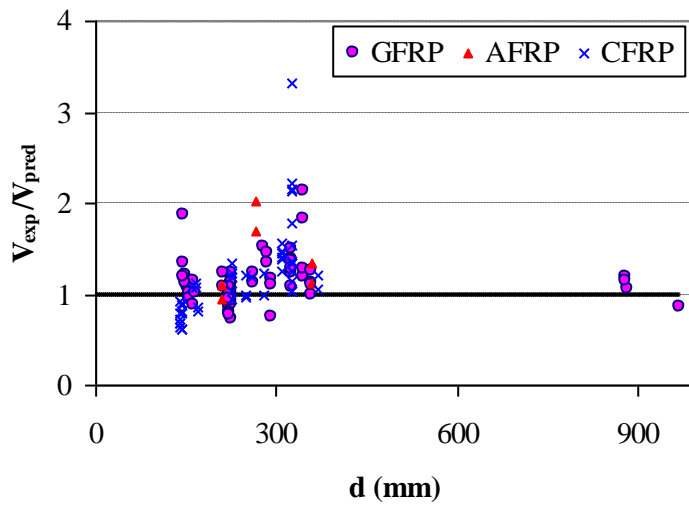
(c) ISIS M03-07



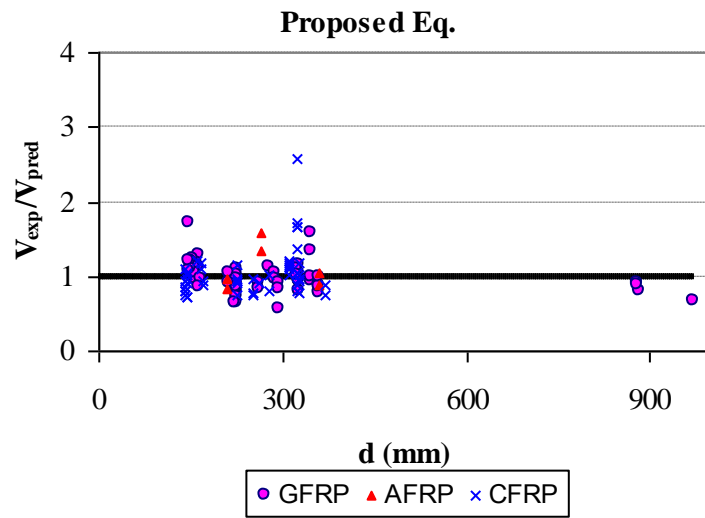
(d) JSCE 97



(e) CNR-DT 203



(f) BISE



(g) Proposed eq.

Figure 7 Experimental to predicted shear capacities versus effective depth of FRP members.

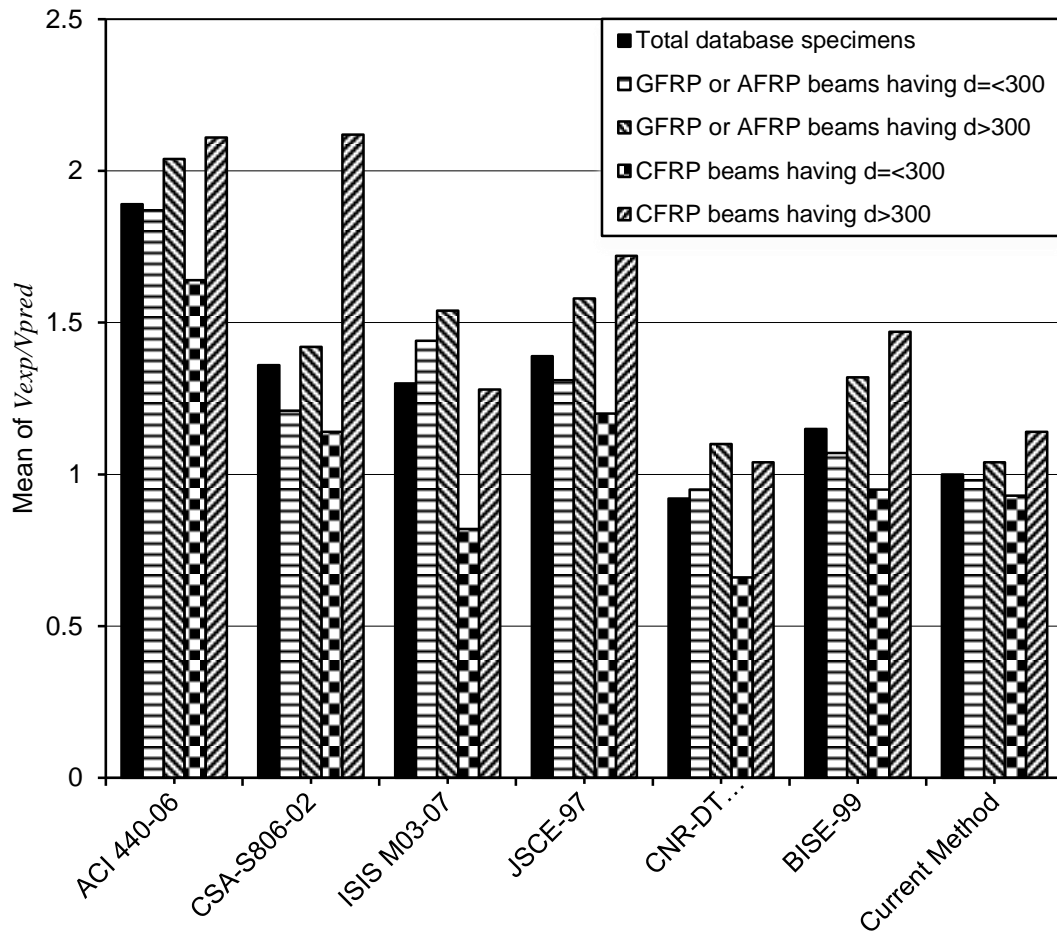


Figure 8 Mean of experimental to predicted shear capacities for various categories of specimens in the database.